Comparison of TID Effects in Space-Like Variable Dose Rates and Constant Dose Rates

Richard D. Harris, *Member, IEEE*, Steven S. McClure, *Member, IEEE*, Bernard G. Rax, Robin W. Evans, and Insoo Jun

***Abstract*—The degradation of the LM193 dual voltage comparator has been studied at different TID dose rate profiles, including several different constant dose rates and a variable dose rate that simulates the behavior of a solar flare. A comparison of results following constant dose rate *vs.* variable dose rates is made to explore how well the constant dose rates used for typical part testing predict the performance during a simulated space-like mission. Testing at a constant dose rate equal to the lowest dose rate seen during the simulated flare provides an extremely conservative estimate of the overall amount of degradation. A constant dose rate equal to the average dose rate is also more conservative than the variable rate. It appears that, for this part, weighting the dose rates by the amount of total dose received at each rate (rather than the amount of time at each dose rate) results in an average rate that produces an amount of degradation that is a reasonable approximation to that received by the variable rate.**

***Index Terms*—Dose Rate, ELDRS, LM193, Solar Flare, TID**

I. Introduction

ENHANCED low dose rate sensitivity (ELDRS) testing on linear bipolar parts is generally performed using Co-60 sources with a constant dose rate, comparing degradation following constant High Dose Rate (HDR, typically ~ 50 rad(Si)/s) exposure for one set of samples with those at constant Low Dose Rate (LDR, typically ~ 0.005–0.01 rad(Si)/s) exposure for another set of identical samples [1]. However, space missions do not see constant dose rates, but rather dose rates that vary throughout the mission; frequently with very significant variations. Examples include lunar or Martian missions where the dose rates are very low except during solar flares when the dose rates are several orders of magnitude larger. In addition, the dose rate during a flare is usually much higher than the dose rate selected for ELDRS study. Other examples include deep space missions where there is very little exposure during the cruise stage, but there may be very high exposure when orbiting a planet, such as Jupiter.

Previous work has shown that for parts that experience ELDRS, the degradation rate increases as the dose rate decreases [2]. For some parts, there does not appear to be a worst case dose rate, or it is so low that it is not practical to perform total ionizing dose (TID) testing in a reasonable amount of time at that low rate. For this reason, hardness assurance methodology has been the subject of many investigations and a number of accelerated test methods have been proposed [3, 4].

ELDRS occurs due to degradation within the transistor base oxide and at the interface between the base oxide and the silicon. Models explaining the phenomena have been reviewed in the past [5 - 7] and more recently [8].

The present study was undertaken to compare the degradation observed in a simulated real variable dose rate profile with the constant dose rates used in most testing. The dose profile of a real solar flare was chosen to provide the alternating dose rate example; in this case the October 1989 flare. The LM193 dual voltage comparator from National Semiconductor was chosen as a representative part as previous work at JPL had shown it to have a strong ELDRS effect [9].

II. Solar Flare Analysis

The October 1989 flare was used as a representative solar flare. The solar proton flux is publically available from the National Oceanic and Atmospheric Administration (NOAA)

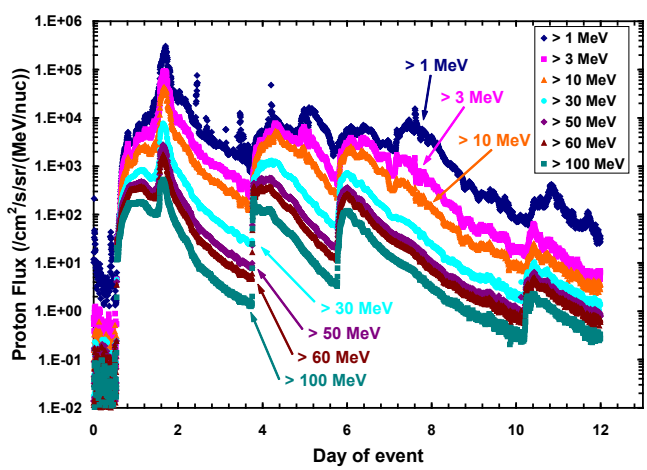

Figure 1. Solar proton flux for the October 1989 flare from the GOES database [6].

Manuscript received July 11, 2008. This work was carried out at the Jet Propulsion Laboratory, California Institute of Technology, under contract with the National Aeronautics and Space Administration (NASA) with funding from the NASA Electronics Parts and Packaging Program (NEPP).

The authors are with the Jet Propulsion Laboratory, California Institute of Technology, Pasadena, CA 91109 USA (richard.d.harris@jpl.nasa.gov; steven.s.mcclure@jpl.nasa.gov; bernard.g.rax@jpl.nasa.gov; robin.w.evans@jpl.nasa.gov; insoo.jun@jpl.nasa.gov)

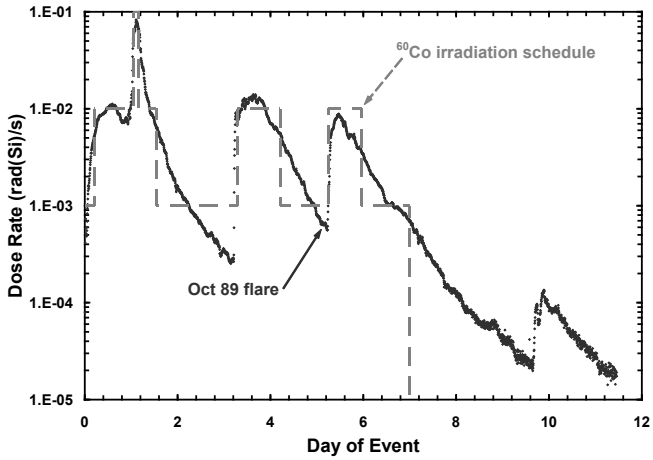

Figure 2. Actual total dose rate *vs.* time for the flare and the simulated dose rate schedule. Dose rate is calculated as that behind 100 mils of Al shielding.

Geostationary Operational Environmental Satellite (GOES) website [10]. The published proton flux *vs.* time is shown in Fig. 1 for this flare. There is quite a bit of interesting structure in the flux as the flare progresses. The time period shown in Fig. 1 covers 12 days, with approximately the first half day being before the flare actually begins.

The dose rate for each time segment was calculated from the proton flux data using the charged particle radiation transport tool NOVICE [11]. The rate calculated in this study is the dose rate behind a thickness of 100 mils of aluminum (Al) shielding, a common baseline shielding for environmental estimates at JPL. The total dose calculated from this procedure is shown in Fig. 2 as the dose rate *vs.* time and in Fig. 3 as the total accumulated dose *vs.* time. The time before the flare began, which we define as a dose rate of $\leq 10^{-4}$ rad(Si)/s, is removed from the data in these figures. The calculated value of the background dose rate before the flare, not shown, is approximately 10^{-6} rad(Si)/s. This background value is actually an upper limit on the background, as the background flux values in Fig. 1 represent instrument sensitivity limits, and not

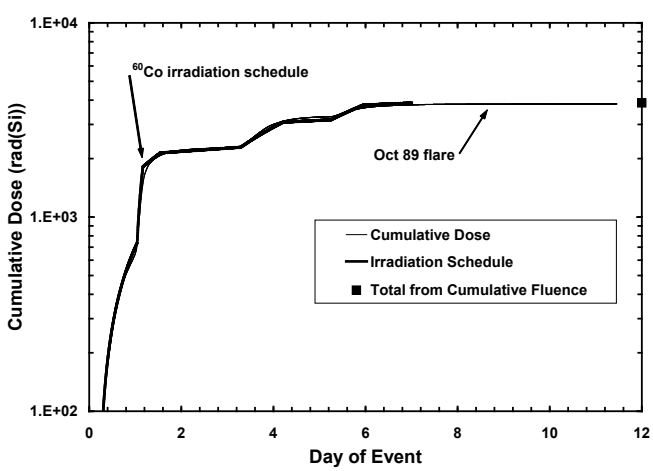

Figure 3. Actual accumulated total dose *vs.* time for the flare and the accumulated dose from the simulated irradiation schedule.

real measured values. As a result, the maximum dose rate during the flare, as seen in Fig. 2, exceeds the background by at least 5 orders of magnitude.

The continuously varying dose rate shown in Fig. 2 is not very practical to implement in the laboratory and so an approximate simulated dose rate schedule was developed from the actual dose rate data. This simulated schedule is also depicted in Fig. 2 (dashed line), and steps between the three different dose rates of 0.001, 0.01, and 0.1 rad(Si)/s. This schedule is a reasonable approximation of the actual dose rate and also results in a good approximation of the total accumulated dose as seen in Fig. 3. Based on the rapidly decreasing dose rate near the end of the flare, as shown in Fig. 2, the simulated schedule was defined to be complete after 7 days. This simulated irradiation schedule gives a total accumulated dose of 3.88 krad(Si) compared to actual total dose of 3.87 krad(Si) depicted in Fig. 3.

III. Experimental Procedure

The device used to compare the degradation under the different dose rate conditions was the LM193 dual voltage comparator from National Semiconductor. The part number for the device tested is LM193J/883, where the J indicates that the part is packaged in an 8-pin ceramic dip. The lot date code for the parts evaluated in this study was 0608. This part choice was made based on previous studies at JPL that showed that the LM193 has a strong ELDRS effect [9]. (It should be noted that this date code precedes the recent announcement of the release of an ELDRS-free LM193 from National Semiconductor.)

Parts were irradiated in the JPL HDR and LDR Co-60 facilities at different dose rates as discussed below. Lead/aluminum (Pb/Al) shields covered the parts during irradiation in accordance with MIL-STD 883, Method 1019.7 [1]. In all cases, the parts were irradiated in an unbiased state (i.e., with the leads shorted together and grounded) as the previous studies at JPL showed that this bias condition produced the largest ELDRS effect [9]. For all data sets, four parts were used for each dose rate condition to allow for statistical variability within the lot of purchased parts and to permit calculation of the standard deviation.

Measurements were performed prior to the irradiation and then at a variety of steps throughout the Co-60 irradiation using an LTS-2020 mixed signal test system. A number of parameters were measured at each step on both channels of the dual comparator. The parameters that showed very large changes were the input bias current ($+I_B$, $-I_B$) and the input offset voltage (V_{OS}). The input bias current showed the largest amount of change during the irradiations and so was singled out to monitor the degradation in this study. The positive input bias current was chosen since its response was similar to the negative input bias.

The total accumulated dose from the flare and the simulated Co-60 schedule is 3.9 krad(Si). This total dose is a little on the low side to see a substantial amount of degradation, either at

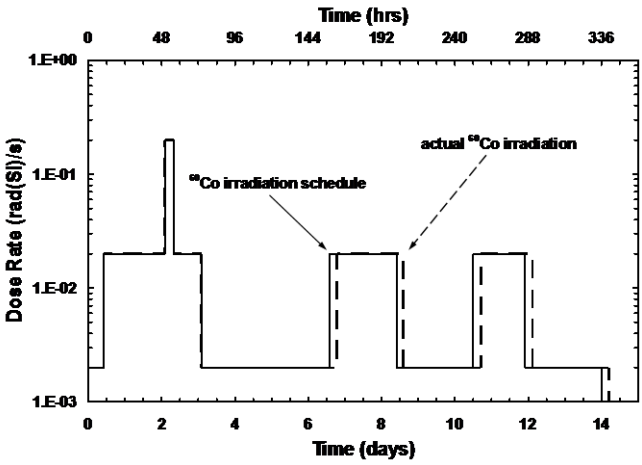

Figure 4. The modified simulated dose rate schedule for the Co-60 irradiation (solid line) and the actual schedule as delivered to the parts (dashed line).

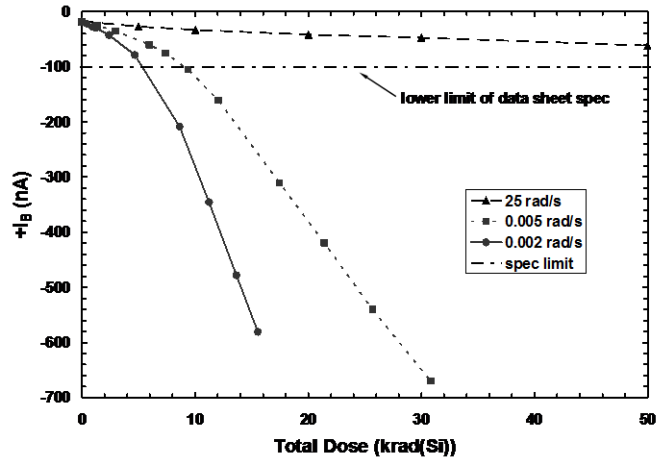

Figure 5. Degradation of $+I_B$ *vs.* total dose for the LM193 for selected dose rates ranging from 25 rad(Si)/s to 0.002 rad(Si)/s showing the very strong ELDRS effect seen in this part.

various steps along the way or at the end. Therefore, the simulated schedule shown in Fig. 2 was modified by doubling the dose rate in each step and doubling the length of each step. In this way, the total simulated accumulated dose was increased to 15.5 krad(Si) while keeping the spirit of the actual flare profile. The modified schedule is shown in Fig. 4 (solid line); along with the actual dose rate profile that the parts received (dashed line). The difference between these two resulted from practical considerations on timing for measurements and dose rate changes.

The modified schedule called for irradiations at dose rates of 0.2, 0.02, and 0.002 rad(Si)/s. The JPL HDR and LDR Co-60 irradiation facilities are both room irradiators. As such, it was possible to obtain each of these dose rates by placing the parts at the appropriate distance from the source. The 0.2 rad(Si)/s irradiation was performed in the HDR facility while the 0.02 and 0.002 rad(Si)/s irradiations were performed in the LDR facility. The appropriate positions were determined by use of an ion chamber dosimeter.

In addition to the variable dose rate schedule, parts were also irradiated at constant dose rate at each of the three different dose rates used in the variable rate schedule. Also, irradiations were carried out at the usual JPL HDR and LDR values; 50 rad(Si)/s and 0.005 rad(Si)/s, respectively.

IV. Experimental Results

A. Constant Dose Rate Results

The degradation of $+I_B$ for several different dose rates is shown in Fig 5. The dose rates shown here are the normal JPL HDR (50 rad(Si)/s), the normal JPL LDR (0.005 rad(Si)/s), and the lowest rate used in this study (0.002 rad(Si)/s). The degradation curves in Fig. 5 demonstrate the very large ELDRS effect that this parameter undergoes.

The lower limit of the $+I_B$ spec from the LM193 datasheet (-100 nA) [12] is also indicated on Fig. 5. At HDR, the parameter is within spec to beyond the edge of the graph (to between 85 and 90 krad(Si)). At LDR it falls out of spec at approximately 9 krad(Si), a very significant change.

It is interesting that the degradation rate is still increasing as the dose rate is lowered from 0.005 to 0.002 rad(Si)/s, and at this lower rate, it is out of spec below 6 krad(Si). Looking at all the data together, there is no sign that the degradation rate is beginning to bottom out even at 0.002 rad(Si)/s. (Indeed, it is observations like this that have led JPL to adopt a standard LDR testing value of 0.005 rad(Si)/s which is below the recommended value of 0.01 rad(Si)/s [1].)

The degradation curves shown in Fig. 5 are unusual for a plot of $+I_B$ degradation. It is generally expected that the degradation will be linear with dose [13]. The non-linear behavior of the $+I_B$ degradation is probably due to the fact that there are two pnp transistors in the input stage of the device as shown in Fig. 6 [12]. Q1 is a substrate pnp and Q2 is a lateral pnp [13]. A lateral pnp generally degrades faster than a substrate pnp, and so an overall non-linear effect is expected.

B. Variable Dose Rate Results

The degradation of $+I_B$ *vs.* dose for the variable dose rate

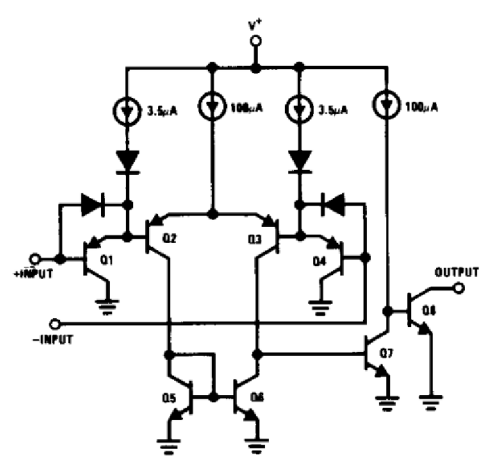

Figure 6. Schematic of LM193 from the manufacturer's datasheet [8].

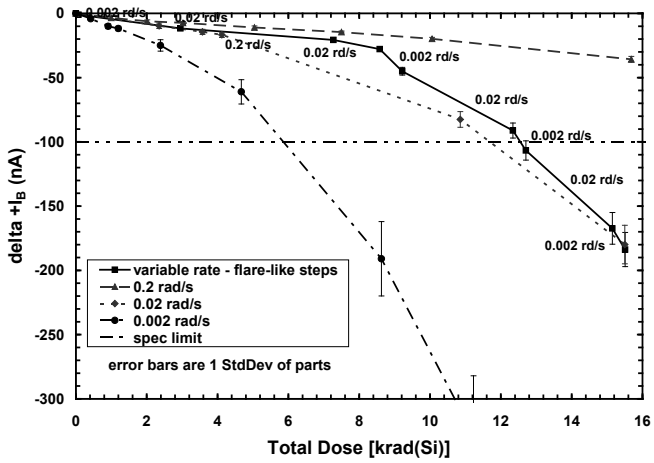

Figure 7. Degradation of $+I_B$ *vs.* dose for the various dose rate conditions; both constant and variable.

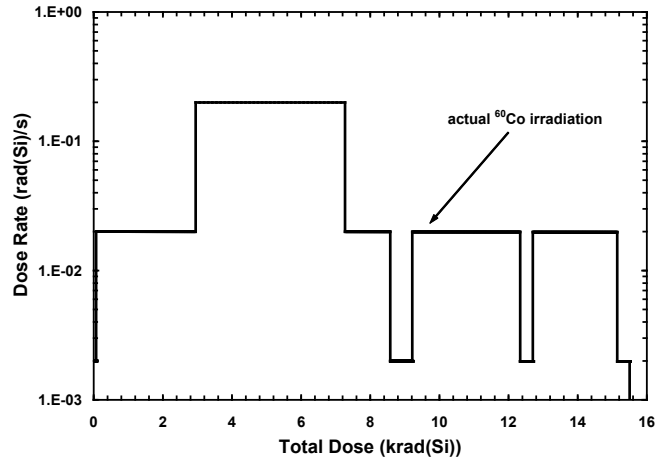

Figure 8. The actual delivered schedule from Fig. 4 replotted with total accumulated dose on the x-axis. This shows the amount of dose received in each dose rate step.

simulated solar flare is shown in Fig. 7. The data is plotted as the average of delta $+I_B$ for the four parts measured. The error bars represent one standard deviation of the measured values for the four parts. Also included in this figure are constant dose rate reference curves for irradiation at 0.2, 0.02, and 0.002 rad(Si)/s, the individual dose rates that make up the simulated variable dose rate schedule.

The overall average dose rate during this irradiation schedule was 0.013 rad(Si)/s (15.5 krad over 14 days). As such, it was expected that the variable curve would lie between the constant 0.002 and 0.02 curves. However, as seen in Fig. 7, the curve exhibits, on average, somewhat less degradation than the 0.02 rad(Si)/s constant dose rate. This is a considerably slower degradation than expected for the average dose rate. It is also very much slower than observed for the lowest constant dose rate of 0.002 rad(Si)/s. As a result, a typical strategy of trying to irradiate at, or near, the lowest dose that will be seen during the mission appears to produce a degradation curve that is very, very conservative.

V. Discussion and Analysis

A. Variable vs. Constant Dose Rate Degradation

Based on the data in Fig. 7, it appears that it may be possible to develop a good model for the amount of degradation expected for a given part by irradiating at a dose rate nearer to the average mission dose rate rather than the lowest dose rate seen during the mission. This would be a big asset in estimating degradation for missions that expect very large dose levels for which testing at the lowest dose rate would take a prohibitively long time.

The actual irradiation schedule of Fig. 4 is replotted in Fig. 8 with the time on the x-axis being replaced with the total accumulated dose. This way of plotting helps make clear how much of the total dose is being received in each step, and therefore how much of the total is received at each dose rate. The total amount of the dose that is received at each of the dose rates is tabulated in Table I.

Almost two-thirds of the dose is received at a dose rate of 0.02 rad(Si)/s. The next biggest contributor is 0.2 rad(Si)/s at a little more than one-quarter. These relative amounts probably explain why the variable dose rate degradation falls between these two constant dose rates since they are the two biggest contributors.

These observations suggest that evaluating each mission profile in detail and determining how much of the total accumulated dose is to be received at each dose rate is needed. From this analysis, it may then be possible to determine a constant dose rate that will approximate the effect of the actual mission. Of course, the actual TID profile that a mission receives is only known in detail after the mission is completed. As a result, it will probably be necessary to evaluate a number of different scenarios to make sure that the worst case possibility is covered.

Before actually implementing such a concept, it will be necessary to test other mission profiles and other part types to see if the trend holds. Then it will be necessary to develop a detailed hardness assurance methodology that will be guaranteed to not underestimate the degradation for different mission types with different types of dose rate profiles. In any case, the results indicate that a test method could be determined for a given mission profile that would result in significant reduction in test time while still being sufficiently conservative to avoid unnecessary mission risk.

Table I
Amount of Dose Acquired at Each Dose Rate

Dose rate (rad(Si)/s)	Dose at that rate (krad(Si))	Percent of total dose (%)
0.2	4.3	28
0.02	9.8	63
0.002	1.4	9

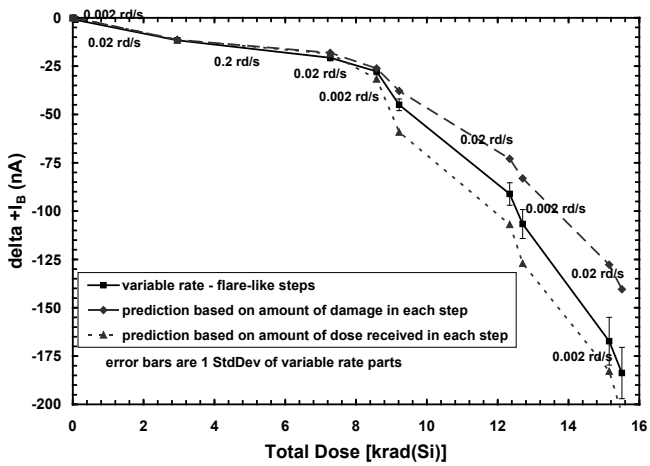

Figure 9. Degradation of $+I_B$ *vs.* dose for the simulated solar flare compared to two models. See text for discussion of the models.

B. *Modeling the Variable Dose Rate Degradation*

Two different models have been developed to try to explain the shape of the degradation curve seen by the variable dose rate schedule. These are depicted in Fig. 9 along with the result of the variable rate irradiation. The data in Fig. 9 is plotted as the amount of degradation; i.e. delta $+I_B$ and the models work with data in this form.

1) *Model 1*

The first model, shown with dashed lines in Fig. 9, is based on the assumption that the damage incurred in each dose rate step is a function of: 1) the amount of damage that has been accumulated up to that point, independent of how that damage was accumulated, and 2) the dose rate in the step under consideration. How the sample got to the level of degradation is not important; only what level it is at and what the dose rate of the next step is.

This was built up by taking the amount of degradation at the initial point of each step and finding the amount of dose required to give that amount of degradation at the dose rate of the upcoming step. Then by adding the amount of dose in the step, the amount of degradation at the end of the step was determined. This was repeated for each step. The degradation at each constant dose rate in Fig. 7 was fit to a third order polynomial that goes through the origin to provide a way of interpolating values between the measured doses.

For example: the variable dose rate starts at 0 degradation and 0.002 rad(Si)/s and extends for 0.072 krad(Si). The fit to the 0.002 rad(Si)/s data predicts a $+I_B$ degradation of -0.576 nA after this dose. The next dose rate is 0.02 rad(Si)/s and extends for 2.88 krad(Si). The fit to this dose rate predicts that a dose of 0.163 krad(Si) will have an initial degradation of -0.576 nA. Added to this dose is the length of irradiation at this dose (0.163 + 2.88) to get an effective final dose of 3.043 krad(Si) which predicts a degradation of -11.907 nA. The next step is at 0.2 rad(Si)/s and the fit to that dose rate which gives an initial degradation of -11.907 nA is 5.453 krad(Si). Added to this is the dose at that rate (4.32 krad(Si)) to get the final predicted value in that step. This process is then repeated throughout the entire dose rate schedule to predict the accumulated damage at each step.

This process produces the dashed curve in Fig. 9. It has the same general shape as the measured degradation curve with appropriate slope changes in each step. Also, the overall values are close to those measured. It is a very intuitive model. There is no reason to expect the part to care how it got to a particular degraded state; only that at the beginning of each step there is certain amount of degradation present and more is then added at during that step at that dose rate.

2) *Model 2*

The second model, shown with dotted lines in Fig. 9, is based on the assumption that the amount of degradation in each step is a function of: 1) the total amount of dose accumulated prior to the beginning of each step, and 2) the dose rate in that step. This model was built up by determining the additional amount of degradation that occurs at constant dose rate for the interval between the initial and final doses at that rate. These additional amounts were then summed to give the accumulated damage at each point.

For example: as in the first model, the variable dose rate starts at 0 degradation and 0.002 rad(Si)/s and extends for 0.072 krad(Si). The fit to the 0.002 rad(Si)/s data predicts a $+I_B$ degradation of -0.576 nA after this dose. For the second step, this model uses the fitted curve to the next dose rate of 0.02 rad(Si)/s to calculate the amount of degradation between total doses of 0.072 and 2.952 krad(Si). These are the actual initial and final total doses for which the variable rate schedule irradiated at 0.02. These values were -0.254 and -11.492 nA, respectively. The change during this step is -11.238 nA which is then added to the value after the previous step (-0.576 nA) to give the total degradation after the first two steps of -11.814 nA. This process is then repeated for each irradiation step and the additional degradation increments are added. As a result, this model depends more on what the starting total doses were for each segment and not the amount of degradation that has previously taken place.

This process produces the dotted curve in Fig. 9. It also has the same general shape as the measured curve with appropriate slope changes in each step. The predicted values are again close to those that are measured. It is not as intuitive as the first model, because it is expected that the amount of previous degradation is more important than the actual dose values; but yet it also produces a close match.

The two models bracket the experimental results as seen in Fig. 9. Both have the correct general shape, with changes in the slope for each of the steps. However, neither fits as well as was hoped. As a result, it is concluded that the degradation does not appear to be explained by a simple combination of the separate degradations in each of the various dose rate steps (Model 1). Apparently, the part maintains some memory of how the previous degradation occurred; i.e. it also remembers the previous dose rates (Model 2).

VI. Conclusions

Device degradation following constant TID dose rate exposure has been compared to that caused by a solar flare-like variable dose rate. Testing at a constant rate equal to the lowest dose rate seen during the simulated flare provides an extremely conservative estimate of the overall amount of degradation. A constant dose rate equal to the average dose rate is also more conservative than the variable rate. It appears that, for this part, weighting the dose rates by the amount of total dose received at each rate (rather than the amount of time at each dose rate) results in an average rate that produces an amount of degradation that is a reasonable approximation to that received by the variable rate.

Two different models have been developed to explain the behavior. The overall degradation does not appear to be explained by a simple combination of the separate degradations in each of the various dose rate steps. Apparently, the part maintains some memory of how the previous degradation occurred; i.e. it also remembers the previous dose rates.

Recommendations for further work include repeating this type of evaluation with different device types and different mission dose profiles.

VII. Acknowledgment

The authors wish to thank A.H. Johnston of JPL for his helpful discussions and suggestions.

References

[1] MIL-STD-883G, Method 1019.7, 2006.

[2] A.H. Johnston, G.M. Swift, and B.G. Rax, "Total dose effects in conventional bipolar transistors and linear integrated circuits," IEEE Trans. Nucl. Sci., vol. 41, no. 6, pp. 2427–2436, Dec. 1994.

[3] R.L. Pease, M. Gehlhausen, J. Krieg, J. Titus, T. Turflinger, D. Emily, and L. Cohn, "Evaluation of proposed hardness assurance method for bipolar linear circuits with enhanced low dose rate sensitivity (ELDRS)," IEEE Trans. Nucl. Sci., vol. 45, no. 6, pp. 2665–2672, Dec. 1998.

[4] J. Boch, F. Saigne, R.D. Schrimpf, J.-R. Vaille, L. Dusseau, S. Ducret, M. Bernard, E. Lorfevre, and C. Chatry, "Estimation of low-dose-rate degradation on bipolar linear integrated circuits using switching experiments," Trans. Nucl. Sci., vol. 52, no. 6, pp. 2616–2621, Dec. 2005.

[5] R.D. Schrimpf, "Physics and hardness assurance for bipolar technologies", 2001 IEEE NSREC Short Course Notebook, Section IV, July 2001.

[6] R.L. Pease, "Total Ionizing Dose Effects in Bipolar Devices and Circuits", IEEE Trans. Nucl. Sci. NS-50, No.3, 539-551, June 2003.

[7] ASTM F1892-04 "Standard guide for ionizing radiation (total dose) effects testing of semiconductor devices", Appendix X2., 2004.

[8] R.L. Pease, R.D. Schrimpf, and D.M. Fleetwood, "ELDRS in bipolar linear circuits: a review", 2008 RADECS conference, Trans. Nucl. Sci., to be published.

[9] C.C. Yui, S.S. McClure, B.G. Rax, J.M. Lehman, T. D. Minto, M.D. Wiedeman, "Total Dose Bias Dependency and ELDRS Effects in Bipolar Linear Devices," 1997 IEEE Radiation Effects Data Workshop Record, pp. 131–137, 1997.

[10] National Oceanic and Atmospheric Administration, National Geophysical Data Center. "SPIDR," Web site, 2008, http://spidr.ngdc.noaa.gov/spidr/

[11] T. Jordan, "NOVICE, A Radiation Transport Shielding Code," Experimental and Mathematical Physics Consultants, Gaithersburg, MD, 2006.

[12] LM193 datasheet at the National Semiconductor website http://www.national.com.

[13] A.H. Johnston, JPL, private communication.